Applied Physics B manuscript No.
(will be inserted by the editor)

Dynamical behaviour of birefringent Fabry-Perot cavities

Paul Berceau[1], Mathilde Fouché[2,3], Rémy Battesti[1], Franck Bielsa[1], Julien Mauchain[1] and Carlo Rizzo[2,3]

[1] Laboratoire National des Champs Magnétiques Intenses (UPR 3228, CNRS-INSA-UJF-UPS), F-31400 Toulouse Cedex, France
[2] Université de Toulouse, UPS, Laboratoire Collisions Agrégats Réactivité, IRSAMC, F-31062 Toulouse, France
[3] CNRS, UMR 5589, F-31062 Toulouse, France

The date of receipt and acceptance will be inserted by the editor

Abstract In this paper we present a theoretical and experimental study of the dynamical behaviour of birefringent cavities. Our experimental data show that usual hypothesis which provides that a Fabry-Perot cavity is a first-order low pass filter cannot explain the behaviour of a birefringent cavity. We explain this phenomenon, and give the theoretical expression of the equivalent cavity filter which corresponds to a second-order low pass filter. Our experimental data show that a birefringent cavity cannot be described as a first-order low pass filter as it is generally assumed. We explain this phenomenon, and give the theoretical expression of the equivalent cavity filter which corresponds to a second-order low pass filter. We also discuss the implications of this cavity behaviour in the case of existing experiments for measuring very low birefringence effects using Fabry-Perot cavities.

1 Introduction

Fabry-Perot cavities are widely used in experiments devoted to the detection of very small optical effects, *e.g.* in the framework of gravitational wave interferometers [1], optomechanical noise studies [2], frequency measurements via optical clocks [3], Lorentz invariance experimental tests [4], or vacuum magnetic birefringence measurements [5,6].

Fabry-Perot cavities made with interferential mirrors are birefringent [7,8,9,10]. For most of the Fabry-Perot fundamental applications, this property can be neglected, at least at first sight, since the studied effects do not depend on polarization. Obviously, this is not the case of birefringence studies reported in refs. [5,6].

The dynamical behaviour of non birefringent cavities has been studied in details [11]. The cavity acts as a first-order low pass filter whatever the polarization of the incident light is, and the frequency spectrum of the transmitted light is modified consequently. As far as we know, nothing has been published so far regarding birefringent cavities. In this paper we present a theoretical and experimental study of the dynamical behaviour of birefringent cavities in the presence of a time variation of the incident light intensity and in the presence of a time variation of the birefringence itself.

Send offprint requests to: mathilde.fouche@irsamc.ups-tlse.fr

2 Experimental Setup

Our study is performed in the framework of the BMV experiment [6] whose goal is to measure vacuum magnetic birefringence. Briefly, as shown on Fig. 1, a linearly polarized Nd:Yag laser beam ($\lambda = 1064\,\mathrm{nm}$) is injected into a Fabry-Perot cavity made of mirrors M_1 and M_2. The length of the cavity is $L = 2.2\,\mathrm{m}$. The laser frequency is locked to the cavity resonance frequency using the Pound-Drever-Hall method [12]. To this end, the laser is phase-modulated at 10 MHz with an electro-optic modulator (EOM). The beam reflected by the cavity is then analyzed on the photodiode $\mathrm{Ph_r}$. This signal is used to drive the acousto-optic modulator (AOM) frequency for a fast control and the Peltier element of the laser for a slow control.

Our birefringence measurement is based on an ellipticity measurement. Light is polarized just before the cavity by the polarizer P. The beam transmitted by the cavity is then analyzed by the analyzer A crossed at maximum extinction and collected by a low noise photodiode $\mathrm{Ph_e}$. The analyzer has an escape window which allows us to extract the reflected ordinary beam. This beam is collected by the photodiode $\mathrm{Ph_t}$. Both signals are simultaneously used in the data analysis as following: $I_\mathrm{e}/I_\mathrm{t} = \sigma^2 + \Psi_\mathrm{tot}^2$, where Ψ_tot is the total ellipticity acquired by the beam going from P to A and σ^2 is the polarizer extinction ratio. Our polarizers are Glan Laser Prism manufactured by Karl Lambrecht Corpora-

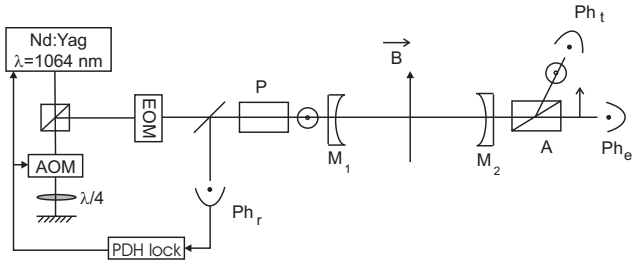

Fig. 1 Experimental setup. A Nd-YAG laser is frequency locked to the Fabry-Perot cavity made of mirrors M_1 and M_2. The laser beam is linearly polarized by the polarizer P and analyzed with the polarizer A. This analyzer allows to extract the extraordinary beam sent on photodiode Ph_e as well as the ordinary beam sent on photodiode Ph_t. The beam reflected by the cavity analyzed on the photodiode Ph_r is used for the cavity locking. A transverse magnetic field B can be applied inside the cavity in order to study the magnetic birefringence of the medium. EOM = electro-optic modulator; AOM = acousto-optic modulator.

tion (Chicago, USA) which have an extinction ratio of 4×10^{-7}.

The origin of the total ellipticity cavity is firstly due to the mirror intrinsic birefringence. Mirrors are similar to wave plates. For small birefringence, combination of both wave plates gives a single wave plate. The phase retardation and the axis orientation of this equivalent wave plate depends on the birefringence of each mirror and on their respective orientation [14,15]. We define the ellipticity induced on the linearly polarized laser beam by the Fabry-Perot cavity as Γ which is set to about 10^{-2} in the experiment described in this paper.

A second component of the total ellipticity appears when a birefringent medium is placed inside the cavity. For example, on magnetic birefringence measurements, a transverse magnetic field B is applied inducing an ellipticity $\Psi \propto B^2 l$ where l is the optical path in the magnetic field.

Finally, if ellipticities are small compared with unity, one gets:

$$I_e/I_t = \sigma^2 + (\Gamma + \Psi)^2. \quad (1)$$

The goal of the experiment presented in this paper is to have a complete understanding of birefringent cavity dynamical behaviour. For this study, two different methods have been implemented. In the next section we present the cavity behaviour in the case of a time variation of the incident light intensity whereas in the last section, the ellipticity inside the cavity is modulated.

3 Time variation of the incident light intensity

In this part, we study the cavity dynamical behaviour to a time variation of the incident laser beam intensity while the total ellipticity remains constant. Two approaches have been used: study of the cavity response to a step function or to an intensity frequency modulation of the incident beam. The first section is devoted to the presentation of both approaches when looking at the ordinary beam collected by Ph_t *i.e.* when the transmitted beam polarization is parallel to the incident one. In the second section, this study is performed on the extraordinary beam *i.e.* when the beam polarization is perpendicular to the incident one.

3.1 Cavity dynamical behaviour towards the ordinary beam

3.1.1 Time response of the cavity to a step function

The simplest way to study the cavity response is to abruptly switch off the intensity of the incident beam locked to the cavity and then to look at the intensity decay of the beam transmitted by the cavity. This method allows to determine typical cavity parameters as the photon lifetime, the cavity finesse, the full width at half maximum or the cavity quality factor.

Experimentally, the intensity is switched off thanks to the acousto-optic modulator (AOM) shown on Fig. 1 and used as an ultrafast commutator. Its switched-off time is less than 1 μs, far less than the photon lifetime as we will see below. On Fig. 2 the intensity of the ordinary beam is plotted as a function of time. For $t < t_0$, the laser is locked to the cavity. The laser intensity is switched off at t_0. For $t > t_0$, one sees the typical exponential decay [13]:

$$I_t(t) = I_t(t_0) e^{-(t-t_0)/\tau}, \quad (2)$$

where τ is the photon lifetime. This lifetime is related to the finesse $F \simeq \pi/(1-R)$ of the cavity through the relation: $\tau = LF/\pi c$ with c the speed of light and R the mirror reflectivity which is supposed to be the same for both mirrors. By fitting our data with this expression one gets $\tau = (245 \pm 10)\,\mu$s corresponding to a finesse of $F = (105 \pm 5) \times 10^3$. The uncertainty results from statistical uncertainty.

3.1.2 Frequency response of the cavity to an intensity modulation

In order to complete our understanding of the experiment, we also study the frequency response of the Fabry-Perot cavity to an intensity modulation. Theoretically, for an incident light modulated in intensity at pulsation ω_F and for a small depth of modulation, the complex response function is given by [11]:

$$H_t(\omega_F) = \frac{I_t^{(\omega_F)}}{I_i^{(\omega_F)}} \propto \frac{1}{1 + i\frac{\omega_F}{\omega_c}}. \quad (3)$$

$I_t^{(\omega_F)}$ ($I_i^{(\omega_F)}$) is the ω_F component of the ordinary (incident) beam intensity. The response function operates as a first-order low pass filter with a cutoff frequency $\nu_c = \omega_c/2\pi = 1/4\pi\tau$.

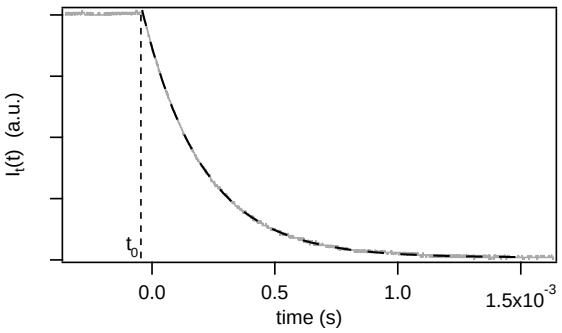

Fig. 2 Time evolution of the intensity of the ordinary beam (gray line). The laser is switched off at $t = t_0$. Experimental data are fitted by an exponential decay (black dashed line) giving a photon lifetime of $\tau = (245 \pm 10)\,\mu$s and a finesse of $F = (105 \pm 5) \times 10^3$.

Experimentally, to study the cavity frequency response, the laser is locked to the cavity and the intensity is modulated with a small depth of modulation thanks to the AOM. The intensity of the incident beam and of the ordinary beam transmitted by the cavity is recorded at different modulation frequencies.

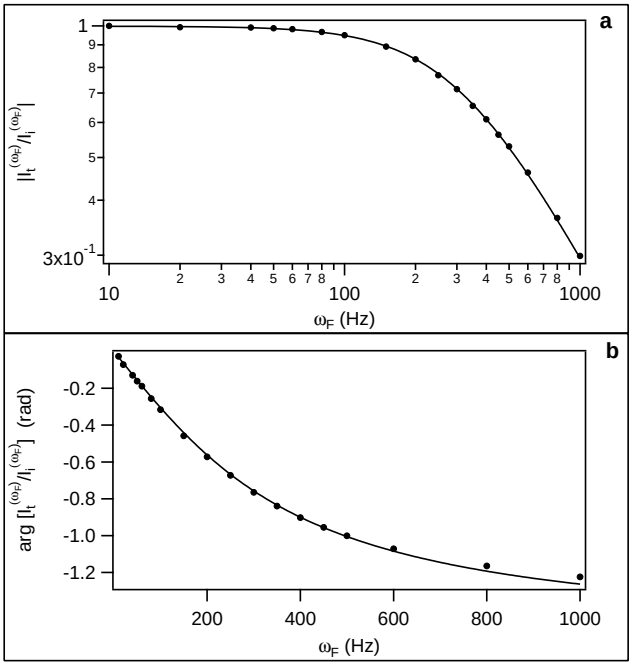

Fig. 3 Experimental cavity response function towards the ordinary beam. (a) Gain of the response function normalized to 1 at low frequency *i.e.* $|I_{\rm t}^{(\omega_{\rm F})}/I_{\rm i}^{(\omega_{\rm F})}|$ as a function of the modulation frequency $\omega_{\rm F}$. Data are fitted by the gain of a first-order low pass filter. (b) Phase delay between $I_{\rm t}^{(\omega_{\rm F})}$ and $I_{\rm i}^{(\omega_{\rm F})}$ as a function of the modulation frequency. Data are fitted by the phase delay of a first-order low pass filter.

Results are presented on Fig. 3. Fig.3a presents the gain of the response function normalized to 1 at low frequency and Fig.3b presents the phase delay. Data are fitted by the response function of a first-order low pass filter. Cutoff frequency is equal to $\nu_{\rm c} = (310 \pm 20)\,$Hz when fitting the gain, and $\nu_{\rm c} = (315 \pm 20)\,$Hz when fitting the phase delay. These values correspond to a finesse of respectively $F = (109 \pm 9) \times 10^3$ and $F = (108 \pm 8) \times 10^3$, which is in agreement with the finesse measured with the previous approach.

While in the second approach we are looking at the frequency response of the cavity, the first approach is performed in the time domain. Both areas of analysis are equivalent and can be connected thanks to Laplace transform. However, the time analysis is usually preferred to the frequency analysis since it is simpler and quicker to implement on the experiment.

Finally, the study performed on the ordinary beam shows that the dynamical behaviour of our cavity is the same as the one obtained on non birefringent cavities. The typical exponential decay is observed when the incident light is suddenly switched off and the frequency response shows that the cavity behaves as a first-order low pass filter.

3.2 Cavity dynamical behaviour towards the extraordinary beam

We now turn to the study on the extraordinary beam collected by $\rm Ph_e$ *i.e.* the beam transmitted by the cavity with a polarization perpendicular to the polarization of the incident one.

3.2.1 Time response of the cavity to a step function

Time evolution of the extraordinary beam when the incident beam is suddenly switched off is shown on Fig. 4. By comparing this curve to the one plotted on Fig. 2, we see that the cavity does not have the same behaviour for $I_{\rm t}$ and $I_{\rm e}$. When one fits $I_{\rm e}$ with an exponential decay, the experimental behaviour is not reproduced and it gives a photon lifetime of $\tau = 735\,\mu$s in disagreement with previously given values. We will show that this is due to the intrinsic birefringence of the cavity.

Let's calculate the transmitted intensity along the round-trip inside the cavity:

– For $t \leq t_0$, the laser is continuously locked to the cavity. According to Eq. (1), the intensities of the ordinary and the extraordinary beams are related by:

$$I_{\rm e}(t \leq t_0) = \Gamma^2 I_{\rm t}(t \leq t_0).$$

The polarizer extinction ratio is neglected since we have $\sigma^2 \ll \Gamma^2$ and no birefringence is applied inside the cavity.

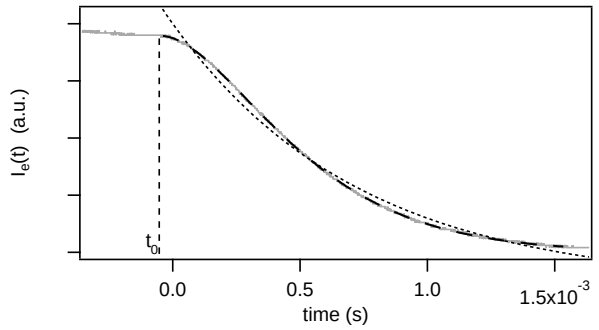

Fig. 4 Time evolution of the intensity of the extraordinary beam (gray line). The laser is switched off at $t = t_0$. Experimental data are fitted by Eq. (5) (black dashed line) giving a photon lifetime of $\tau = (245 \pm 10)\,\mu$s. The fit with an exponential decay (dots) does not correspond to the experimental behaviour and gives a photon lifetime of $\tau = 735\,\mu$s in disagreement with previously given values.

– At $t = t_0$, the laser beam is abruptly switched off, the cavity empties gradually. The ordinary and extraordinary beams are slightly transmitted at each reflection on the mirrors. But, because these mirrors are birefringent, some photons of the ordinary beam are converted into the extraordinary one. The reverse effect is neglected because $I_\mathrm{e} \ll I_\mathrm{t}$.
As shown on Eq. (1), the total ellipticity corresponds to the sum of ellipticities when they are small. Furthermore, following Ref. [15], the ellipticity Γ induced by the cavity is related to the ellipticity induced per round-trip γ trough the relation: $\gamma = \Gamma\pi/F$.
Thus after one round-trip inside the cavity, *i.e.* at time $t_0 + t_\mathrm{D} = t_0 + 2L/c$, we get:

$$I_\mathrm{e}(t_0 + t_\mathrm{D}) = (\Gamma + \gamma)^2\, I_\mathrm{t}(t_0 + t_\mathrm{D}).$$

– After p round-trips, one gets the intensity of the extinction beam:

$$I_\mathrm{e}(t_0 + pt_\mathrm{D}) = (\Gamma + p\gamma)^2\, I_\mathrm{t}(t_0 + pt_\mathrm{D}). \qquad (4)$$

Assuming that Eq. (4) holds not only at times $t_0 + pt_\mathrm{D}$ but also at any time $t > t_0$ and using Eq. (2) for I_t, we can write:

$$I_e(t) = I_e(t_0)\left(1 + \frac{t - t_0}{2\tau}\right)^2 e^{-\frac{t-t_0}{\tau}}. \qquad (5)$$

This expression is used to fit our experimental data plotted on Fig. 4. We find a photon lifetime of $\tau = (245 \pm 10)\,\mu$s which is in good agreement with the value found in the previous section.

3.2.2 Frequency response of the cavity to an intensity modulation

As done before, we also study the frequency response of the cavity towards the extraordinary beam to an intensity modulation. Results are presented on Fig. 5.

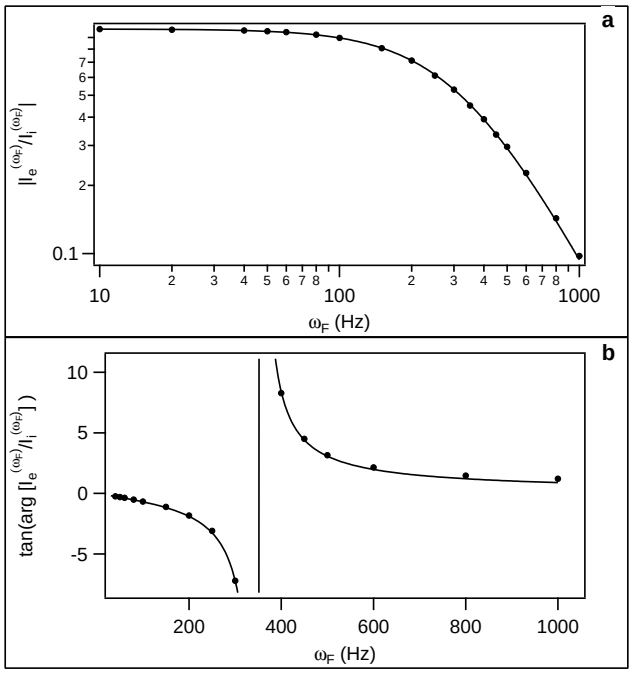

Fig. 5 Cavity response function towards the extraordinary beam. (a) Gain of the response function normalized to 1 at low frequency *i.e.* $|I_\mathrm{e}^{(\omega_\mathrm{F})}/I_\mathrm{i}^{(\omega_\mathrm{F})}|$ as a function of the modulation frequency ω_F. Data are fitted by the gain of a second-order low pass filter. (b) Tangent of the phase delay between $I_\mathrm{e}^{(\omega_\mathrm{F})}$ and $I_\mathrm{i}^{(\omega_\mathrm{F})}$ as a function of the modulation frequency. Data are fitted by the phase delay of a second-order low pass filter.

To calculate the complex response function expected theoretically, we use Eq. (5) and the Laplace transform and we get:

$$H_\mathrm{e}(\omega_\mathrm{F}) = \frac{I_\mathrm{e}^{(\omega_\mathrm{F})}}{I_\mathrm{i}^{(\omega_\mathrm{F})}} \propto \left(\frac{1}{1 + i\frac{\omega_\mathrm{F}}{\omega_\mathrm{c}}}\right)^2.$$

$I_\mathrm{e}^{(\omega_\mathrm{F})}$ corresponds to the ω_F component of the extraordinary beam intensity. The response function operates as a second-order low pass filter with the same cutoff frequency ν_c found previously for the ordinary beam. Data of Fig. 5 are fitted by the following expressions:

$$|H_\mathrm{e,n}(\omega_\mathrm{F})| = \frac{1}{1 + \left(\frac{\omega_\mathrm{F}}{\omega_\mathrm{c}}\right)^2} \qquad (6)$$

$$\arg[H_\mathrm{e,n}(\omega_\mathrm{F})] = -\frac{2\frac{\omega_\mathrm{F}}{\omega_\mathrm{c}}}{1 - \left(\frac{\omega_\mathrm{F}}{\omega_\mathrm{c}}\right)^2}. \qquad (7)$$

Cutoff frequencies given by the fits are $\nu_c = (325 \pm 20)$ Hz and $\nu_c = (350 \pm 20)$ Hz and are consistent with the values found in the previous section.

The study presented in this part shows that a birefringent cavity cannot be described as a first-order low

pass filter as it is generally assumed for usual cavities. For the extraordinary beam, the cavity acts as a second-order low pass filter instead of a first-order. This filter represents the combined action of two successive first-order low pass filters. While the first filter characterizes the usual cavity behaviour as seen in section 3.1, we can interpret the second filter in terms of pumping or filling: due to the mirror birefringence, some photons of the ordinary beam are gradually converted into the extraordinary beam at each reflection.

4 Time variation of the birefringence

The second method implemented to study the cavity dynamical behaviour consists in varying the cavity birefringence itself. The intrinsic cavity birefringence can hardly be modulated. We have chosen to obtain a time variation of the cavity birefringence by a variation of the birefringence of the medium placed inside the cavity.

According to Eq. (1), the measured signal is given by:

$$I_{\mathrm{e}}(t)/I_{\mathrm{t}} = \sigma^2 + \Gamma^2 + 2\Gamma\Psi(t).$$

We assume that $\Psi \ll \Gamma$. Let's consider that the ellipticity per round-trip ψ applied inside the cavity is modulated with a pulsation ω_{F}:

$$\psi(t) = \psi_0 \sin(\omega_{\mathrm{F}} t).$$

Following calculations performed in [6], the ellipticity outside of the cavity induced by the applied birefringence is:

$$\Psi(t) = \frac{\Psi_0}{\sqrt{1 + \left(\frac{\omega_{\mathrm{F}}}{\omega_{\mathrm{c}}}\right)^2}} \sin(\omega_{\mathrm{F}} t + \phi) \qquad (8)$$

with $\tan\phi = -\omega_{\mathrm{F}}/\omega_{\mathrm{c}}$ and $\Psi_0 = \psi_0 F/\pi$. We see that this ellipticity corresponds to an ellipticity filtered by a first-order low pass filter with a cutoff frequency corresponding to the one of the cavity. In other words, if the ellipticity ψ varies over the photon lifetime in the cavity, the ellipticity outside of the cavity is attenuated and does not remain in phase with ψ.

From the experimental point of view, the birefringence inside the cavity corresponds to a magnetic birefringence. The induced ellipticity per round-trip is given by: $\psi \propto B^2 \sin 2\theta$ where θ is the angle between light polarization and the direction of the transverse magnetic field. To modulate this ellipticity, one can modulate the value of the magnetic field or modulate the direction of the magnetic field.

On our experiment, the magnetic field is created thanks to pulsed coils. Thus, the time variation of the applied birefringence corresponds to a time variation of the square of the magnetic field. On Fig. 6a, a typical magnetic pulse is plotted. It reaches its maximum of 2.9 T within less than 2 ms.

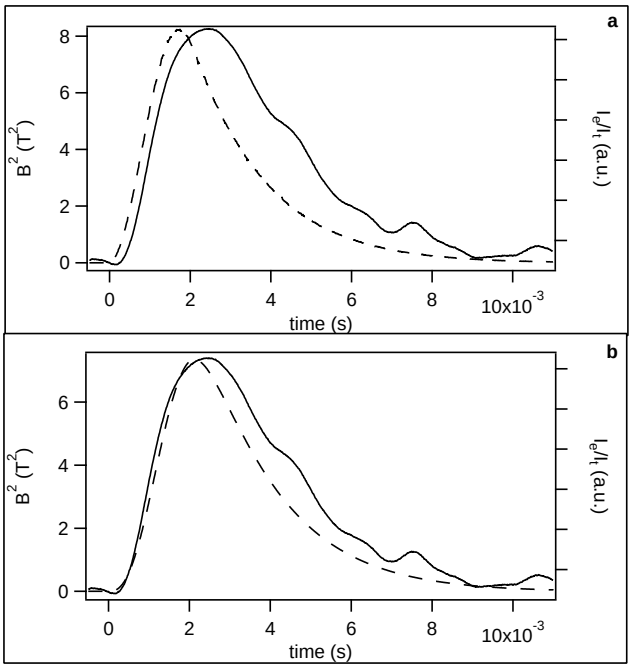

Fig. 6 (a) Dashed curve: Square of the magnetic field as a function of time. Line: Signal $I_{\mathrm{e}}/I_{\mathrm{t}}$ as a function of time while the laser is locked to the cavity. (b) Dashed curve: Square of the magnetic field filtered by a first-order low pass filter corresponding to the cavity filtering. Line: Signal $I_{\mathrm{e}}/I_{\mathrm{t}}$ as a function of time while the laser is locked to the cavity. Shift of both maxima are compensated when the cavity filtering is taken into account. Noise observed on the transmitted intensities after 2 ms of magnetic pulse are due to vibrations induced on the cavity by the magnetic pulse. This part is not taken into account in the data analysis.

The cavity finesse is 100000 which corresponds to a photon lifetime of 230 ms. About 15 mbar of air was inserted inside the vacuum chamber which contains the cavity and the polarizers. The applied birefringence is always smaller compared to the mirror birefringence. The observed signal is shown on Fig. 6a and b on the right axis and compared to the magnetic field. We see that both maxima of B^2 and $I_{\mathrm{e}}/I_{\mathrm{t}}$ do not coincide. But as expected by Eq. (8) and shown on Fig. 6b, this shift is actually compensated if we apply a first-order low pass filter corresponding to the cavity filtering on the square of the magnetic field.

Finally, the value of the magnetic birefringence is calculated through the correlation between $\Psi(t)$ and $B^2(t)$ filtered [6]. In the case of Fig. 6 this analysis is not performed for $t > 2$ ms where vibrations are induced on the cavity due to the magnetic pulse. Improvements are currently under development to minimize this effect. If the filter is not applied on the magnetic field *i.e.* if the cavity influence is not taken into account, a systematic uncertainty of a few percents is added on the value of the magnetic birefringence.

5 Conclusion

We have studied the dynamical behaviour of birefringent Fabry-Perot cavities. Actually, because of the intrinsic mirror birefringence all Fabry-Perot cavities are birefringent, and our study applies to all of them. We have shown that the cavity dynamical behaviour depends on polarization.

For intensity modulation of the incoming beam, its frequency spectrum is filtered by the cavity differently depending on the polarization of the light exiting the cavity. This filtering also applies to the intensity noise frequency spectrum.

We have also considered the case of a cavity birefringence time variation. To study how a cavity filters such a modulation, we have measured a magnetic birefringence induced by a pulsed magnetic field on a medium inside a Fabry-Perot cavity. We have experimentally shown that depending on the photon lifetime in the cavity *i.e.* the cavity cutoff frequency, the induced ellipticity is attenuated and becomes out of phase with respect to the magnetic field pulse. The finesse of the cavity we used is of the order of 100000. A higher finesse will correspond to a more important filtering and to a bigger systematic uncertainty correction.

The problem is exactly the same if the value of the magnetic field remains fixed while its direction compared to the cavity birefringence axis is rotated as it is the case on other experiments measuring magnetic birefringence. For example, in ref.[16] where the Cotton-Mouton effect in helium is measured, a superconducting dipole magnet rotating at a frequency of $0.35\,Hz$ is used. The finesse is 100000 corresponding to a cavity cutoff frequency of $\nu_c = 116.5\,\mathrm{Hz}$. Taking into account the cavity filtering allows to avoid a systematic uncertainty of $1.8\times10^{-3}\,\%$ on the final magnetic birefringence. In the same way, in ref. [17], where the Cotton-Mouton effect of different gases is measured, a dipole permanent magnet is rotating at about 6.8 Hz inside a cavity with a cutoff frequency of 725 Hz. The systematic uncertainty is then $1.7\times10^{-2}\,\%$. Systematic uncertainty on such experiments is negligible compared to statistical uncertainties, but it will become more important if the rotating frequency increases and/or the cavity finesse increases.

6 Acknowledgements

This work has been performed in the framework of the BMV project. We thanks all the members of the BMV collaboration, and in particular Hugo Bitard, G. Bailly and M. Nardone. We acknowledge the support of the *ANR-Programme non thématique* (ANR-BLAN06-3-139634), and of the *CNRS-Programme National Particule Univers.*

References

1. M. Rakhmanov, F. Bondu, O. Debieu and R.L. Savage Jr, Class. Quantum Grav. **21**, S487 (2004); T. Akutsu *et al*, Class. Quantum Grav. **23**, S23-S28 (2006); D.E. McClelland *et al*, Class. Quantum Grav. **23**, S41-S49 (2006); H. Lück *et al*, Class. Quantum Grav. **23**, S71-S78 (2006); The Virgo collaboration, Appl. Opt. **46**, 3466-3484 (2007)
2. P. Verlot, A. Tavernarakis, T. Briant, P.F. Cohadon, A. Heidmann, Phys. Rev. Lett. **102**, 103601 (2009)
3. B. Young *et al*, Phys. Rev. Lett. **82**, 3799-3802 (1999); T. Nazarova *et al*, Appl. Phys. B **83**, 531536, (2006); A.D. Ludlow *et al*, Opt. Lett. **32**, 641643 (2007); S.A. Webster *et al*, Phys. Rev. A **75**, 011801 (2007); J. Millo *et al*, Phys. Rev. A **79**, 053829 (2009)
4. C. Eisele, A.Y. Nevsky, S. Schiller, Phys. Rev. Lett. **103**, 090401 (2009)
5. S.-J. Chen, H.-H. Mei, and W.-T. Ni, Mod. Phys. Lett. A **22**, 2815-2831 (2007); E. Zavattini, G. Zavattini, G. Ruoso, G. Raiteri, E. Polacco, E. Milotti, V. Lozza, M. Karuza, U. Gastaldi, G. Di Domenico, F. Della Valle, R. Cimino, S. Carusotto, G. Cantatore, and M. Bregant, Phys. Rev. D **77**, 032006 (2008)
6. R. Battesti, B. Pinto Da Souza, S. Batut, C. Robillard, G. Bailly, C. Michel, M. Nardone, L. Pinard, O. Portugall, G. Trénec J.-M. Mackowski, C.L.J.A. Riken, J. Vigué and C. Rizzo, Eur. Phys. J. D **46**, 323-333 (2008)
7. F. Bielsa, A. Dupays, M. Fouché, R. Battesti, C. Robilliard and C. Rizzo, Appl. Phys. B **97**, 457-463 (2009) and references therein
8. J.Y. Lee, H.-W. Lee, J.W. Kim, Y.S. Yoo and J.W. Hahn, Appl. Opt. **39**, 1941-1945 (2002)
9. J. Morville and D. Romanini, Appl. Phys. B **74**, 495-501 (2002)
10. H. Huang and K.K. Lehmann, Appl. Opt. **47**, 3817-3827 (2008)
11. N. Uehara and K. Ueda, Appl. Phys B. **61**, 9-15 (1995)
12. R.W.P. Drever, J.L. Hall, F.V. Kowalski, J. Hough, G.M. Ford, A.J. Munley and H. Ward, Appl. Phys. B **31**, 97-105 (1983)
13. O. Svelto, *Principles of lasers* (Springer, 4th edition, 1998), pp. 167-168
14. D. Jacob, M. Vallet, F. Bretenaker, A. Le Floch, Opt. Lett., **20**, 671-673 (1995)
15. F. Brandi, F. Della Valle, A.M. De Riva, P. Micossi, F. Perrone, C. Rizzo, G.Ruoso and G. Zavattini, Appl. Phys. B **65**, 351-355 (1997)
16. M. bregant *et al*, Chem. Phys. Lett. **471**, 322-325 (2009)
17. H.-H. Mei, W.-T. Ni, S.-J. Chen and S.-S. Pan, Chem. Phys. Lett. **471**, 216-221 (2009)